European Conference on Computational Fluid Dynamics
ECCOMAS CFD 2006
P. Wesseling, E. Oñate and J. Périaux (Eds)


# COMPUTATION OF TOPOLOGICAL SENSITIVITIES IN FLUID DYNAMICS: COST FUNCTION VERSATILITY

**Carsten Othmer*, Thomas Kaminski† and Ralf Giering†**

*Volkswagen AG, Numerical Analysis E1, Letter Box 1697, D-38436 Wolfsburg
e-mail: carsten.othmer@volkswagen.de
†FastOpt, D-20357 Hamburg, http://www.FastOpt.com

**Key words:** CFD, Topology Optimization, Adjoint Methods, Automatic Differentiation

**Abstract.** *Topology optimization of fluid dynamical systems is still in its infancy, with its first academic realizations dating back to as late as three years ago. In this paper, we present two approaches to fluid dynamic topology optimization that are based on potential flows and adjoint states, respectively. Special emphasis is paid to the computation of topological sensitivities with discrete adjoints and its versatility with respect to changes of the cost function: After providing the proof of concept of a discrete adjoint-based methodology for the optimization of dissipated power, we compute sensitivities with respect to equal mass flow through different outlets, flow uniformity and also angular momentum of the flow in the outlet plane.*

## 1 TOPOLOGY OPTIMIZATION IN FLUID DYNAMICS

In structure mechanics, topology optimization is a well-established concept for design optimization with respect to tension or stiffness [1]. Its transfer to computational fluid dynamics (CFD), however, just began three years ago with the pioneering work of Borrvall and Petersson [2].

Starting point for fluid dynamic topology optimization is a volume mesh of the entire installation space. Based on a computation of the flow solution inside this domain, a suitable *local* criterion is applied to decide whether a fluid cell is "good" or "bad" for the flow in terms of the chosen cost function. Two lines of thought have developed on how to iteratively remove the identified bad cells from the fluid domain: The cells are either punished via a momentum loss term [2]-[6], or holes are inserted into the flow domain, with their positions being determined from an evaluation of the topological asymptotic [7, 8].

Obviously, topology optimization fits ideally into the common industrial design process of freeform geometries. It delivers an unbiased design from scratch and, since it starts from the feasible domain and only *removes* fluid cells, design domain restrictions are automatically fulfilled. Possible automotive applications are the optimization of air ducts

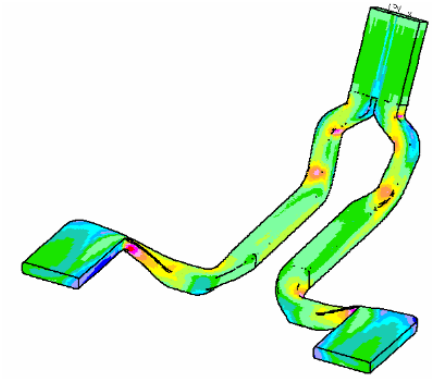

Figure 1: Typical air duct for rear seat ventilation. Air from the ventilator enters the channel (top right) and leaves it through the two outlets. Colours indicate the velocity magnitude.

for cabin ventilation, which are usually subject to severe spatial design restrictions (see Fig. 1 for an example), or of engine intake ports with respect to the swirl motion of the outgoing air. However, due to the lack of a professional tool, especially for the industrially relevant high-Reynolds-number flows, topology optimization has not yet entered the regular design process. In this paper, we present a methodology that has the potential of a straightforward implementation into a professional CFD solver. It uses a discrete adjoint approach to compute sensitivities with respect to the chosen cost function. We introduce this method as an extension of a pragmatic approach to be discussed in the following, and we verify its applicability to a variety of cost functions.

## 2 APPROACHES PURSUED AT VOLKSWAGEN

Similar to topology optimization in structure mechanics its fluid dynamic counterpart is also a discrete 0-1 problem: Either a cell belongs to the fluid domain or it does not. In order to render the transition between these two extreme states continuous, the design domain is treated as a porous medium: Each cell is assigned an individual porosity $\alpha_{ijk}$, which is modelled via Darcy's law. The value of $\alpha_{ijk}$ determines if the cell is fluid-like (low porosity values) or has a rather solid character (high values of $\alpha_{ijk}$). In other words, the porosity field controls the geometry, and the $\alpha_{ijk}$ are the actual design variables.

Once the design variables are determined, the central element of any topology optimization methodology is to compute their sensitivities, i. e. the partial derivative of the cost function with respect to the chosen design variables. For the computation of sensitivities we investigated two different methods that will be discussed in the following subsections. The obtained sensitivities can then be plugged into a gradient-based optimization algorithm – possibly with some penalization of intermediate porosity values in order to enforce a "digital" porosity distribution. After several iterations, the desired optimum topology is finally extracted as an isosurface of the obtained porosity distribution or simply as the collection of all non-porous cells.

### 2.1 A pragmatic methodology

Our pragmatic way of computing appropriate sensitivities was motivated by the design requirements of climate channels: They have to duct a given mass flow from inlet to outlet with the least possible energy loss. If present in the flow, backflow structures, such as dead water regions, usually account for a large fraction of the energy loss. Hence, their elimination or at least reduction constitutes a straightforward, albeit indirect, way of optimizing the geometry of climate channels with respect to their energetic efficiency.

The open question is, of course, how to define a local physical criterion that allows to *identify* the regions of backflow. And the answer is as simple as this: by comparison of the actual flow situation with a velocity field that – by definition – does not exhibit any backflow region, namely a *potential flow*. This potential flow $\vec{v}_{pot} = -\nabla\phi$ can be computed by solving the Laplace equation

$$\Delta\phi = 0 \tag{1}$$

with appropriate boundary conditions.

The zero vorticity of potential flows implies that the flow direction is everywhere "from inlet to outlet". It is this feature that allows to easily identify dead water regions in the flow field: Where the actual velocity direction deviates substantially from the one of the corresponding potential flow, e. g. by more than 90 degrees, there must be a backflow region! Hence, the scalar product $\vec{v} \cdot \vec{v}_{pot}$ of actual velocity $\vec{v}$ and potential velocity $\vec{v}_{pot}$ suggests itself as a sensible choice for the sensitivity that we were looking for: (1) The transition between "good" cells and "bad" cells occurs at a deviation of 90 degrees, and (2) being proportional to the magnitude of the actual velocity, this sensitivity definition takes into account the relative importance of the respective cell.[1]

Fig. 2 shows the application of this sensitivity definition to a simple two-dimensional (2D) test case with $100 \times 100$ Cartesian grid cells. At a Reynolds number of 2500 the flow enters the box with a prescribed uniform velocity profile through an inlet in the south wall and leaves it through a zero-pressure outlet in the east wall. We started from zero porosity and used the sensitivities to update the porosity field according to a steepest descent step:

$$\alpha^{new} = \alpha^{old} - \lambda\, \vec{v} \cdot \vec{v}_{pot}\,. \tag{2}$$

For the sake of simplicity, the stepsize $\lambda$ was kept fixed, i. e. no line-search was performed. For this test application, we closely coupled the CFD iterations with the porosity update, similar to what is usually referred to as "one-shot method": After each inner CFD iteration, the porosity field was updated according to Eqn.(2).

[1] As will actually be demonstrated in a parallel study [9], the exact sensitivity for cost functions like total pressure drop or dissipated power is the scalar product of real – or, better, primal – velocity and adjoint velocity. Hence, $\vec{v} \cdot \vec{v}_{pot}$ is a good choice for the sensitivity not only on the basis of physical reasoning, but can also be understood in terms of approximating the adjoint flow field by a potential flow.

Four stages of this procedure are shown in Fig. 2. The employed CFD solver starts from a potential flow field and then begins to develop the regions of vorticity – first adjacent to the inlet region (Fig. 2a) and later on all along the bended flow path. Our way of updating the porosity, however, effectively inhibits the build-up of vorticity and ends up in a stationary flow field that does not contain any backflow (Fig. 2d). The "optimum" channel shape was extracted from the obtained porosity field by collecting all non-porous cells, and was shown in a separate computation (with a real no-slip boundary condition along the channel walls) to be superior to the initial box geometry by around 15% in dissipated power.

Two things make this method extremely fast: (1) As mentioned above, the CFD iterations and the porosity update are closely coupled, and (2) since the porosity update is chosen such that the development of vortex structures is inhibited, no computing time has to be spent on resolving the details of these regions. As a result, the overall topology optimization takes less time than a single CFD computation of the original flow domain!

This method was shown to produce good results also for 3D cases (e. g. Fig. 6 in [10]). By construction, it generates a geometry without backflow regions. Albeit indirect, this allows for significant improvements of climate channel designs – but, and this is the major shortcoming of this method, only for cost functions like dissipated power or pressure drop. For other design objectives that are commonly encoutered in engineering optimization problems, like flow uniformity or swirl motion, our pragmatic approach is simply not applicable. That is why we did not pursue it any further, but rather set out to compute "real" sensitivities on the basis of adjoint states.

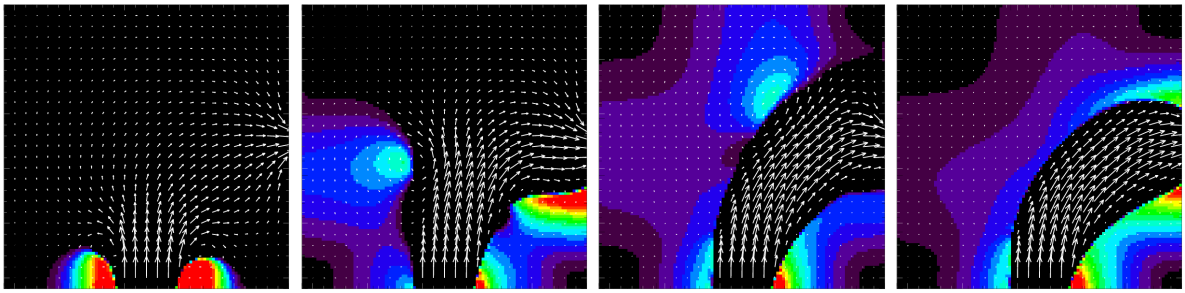

(a) (b) (c) (d)

Figure 2: Pragmatic approach in a one-shot fashion: Porosity distribution at four stages during the development towards a steady state. Note the localized areas of high porosity in regions of increased backflow.

### 2.2 A discrete adjoint approach

For a proof of concept of discrete adjoint-based topology optimization, we used Pruett's Fortran90 version [11] of Griebel's 2D incompressible Navier-Stokes solver NaSt2D [12]. A Darcy term to account for porosity was added, and we implemented a cost function corresponding to the dissipated power $E$

$$E = -\int_{\partial\Omega} p_t \vec{v} \cdot d\vec{A}, \tag{3}$$

with $\Omega$, $p_t$ and $\vec{v}$ being the flow domain, the total pressure and the flow velocity, respectively. The resulting code was then transformed by the automatic differentiation (AD) tool TAF (Transformation of Algorithms in Fortran [13]) to a highly efficient adjoint derivative code (see [14] for details of the differentiation process and code performance). It allows to elegantly compute the sensitivities of the design variables with respect to the chosen cost function, in other words the partial derivatives $\partial E/\partial \alpha_{ijk}$.

Fig. 3 illustrates the application of this code to the 2D box example of the previous subsection: For the original flow field as shown in Fig. 3a, the sensitivities of the "good" cells (i. e. those with negative sensitivities) and the "bad" or counterproductive cells are displayed separately in Figs. 3b and c. As expected, the most important cells for the flow passage lie along the main path, whereas the counterproductive cells are mostly located in the backflow regions. Fig. 3d finally displays the flow field that was obtained after five unpenalized steepest descent iterations of porosity update. It constitutes a cost function improvement of 25% as compared to the original flow field.

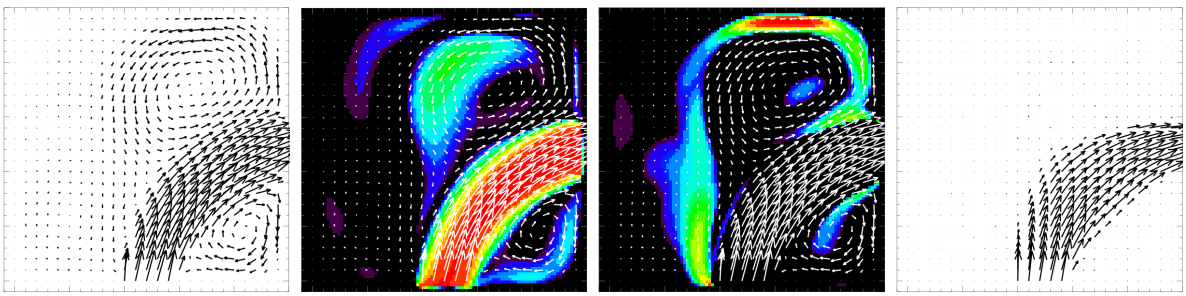

(a) (b) (c) (d)

Figure 3: Adjoint approach applied to the 2D example of Fig. 2: (a) Initial velocity field, (b) sensitivities of "good" cells, (c) sensitivities of "bad" cells, (d) velocity field after five iterations.

## 3 ADJOINT APPROACH: COST FUNCTION VERSATILITY

As stated above, the motivation behind developing an *adjoint-based* topology optimization methodology was the cost function versatility of such a method. The remainder of the paper is therefore dedicated to verifying the performance of the method for a set of different objective functions. To that end, the primal code was extended to three dimensions, and an adjoint derivative code was again obtained via AD with TAF.

In this context, it is worth bringing to mind one of the big advantages of using AD for the generation of adjoint code: Extensions to the suite of objective functions can be made in a practically automatic fashion. For each of the three new objective functions (subroutines of about 100 lines of Fortran) tangent and adjoint derivative codes were updated and verified by TAF within turnaround times of less than 24 hours.

### 3.1 Dissipated power

For a 3D segment of the climate channel of Fig. 1 we computed the sensitivities wrt. dissipated power (Fig. 4). Hot colours correspond to negative sensitivities, whereas the dark blue areas mark the counterproductive cells. The white contours are the isolines of zero sensitivities, i. e. the borderline between good and bad cells. As could be expected from physical reasoning, the counterproductive cells are located in the regions of detachment and backflow.

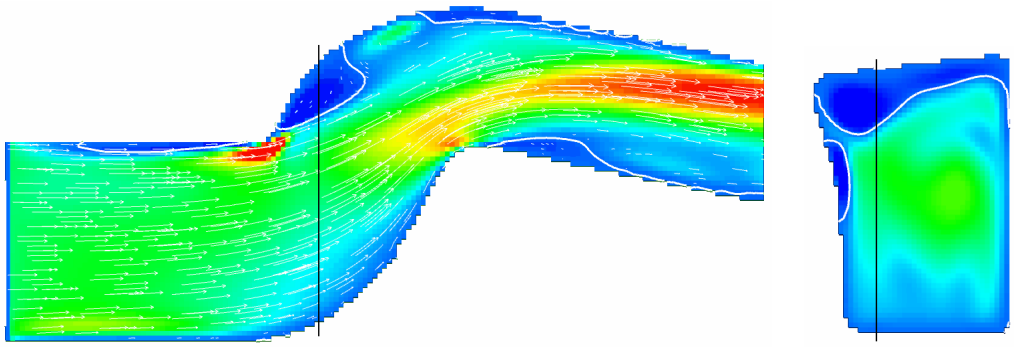

Figure 4: Sensitivities wrt. dissipated power for a segment of the air duct of Fig. 1: The air enters the channel from the left hand side at a Reynolds number of 2500. Hot and cold colours correspond to good and bad cells, respectively. Isolines of zero sensitivity are shown in white.

### 3.2 Flow uniformity

Apart from the dissipated power, the uniformity of the flow upon leaving the outlet plane is an important design criterion of air ducts. It is related to the efficiency of distributing fresh air inside the car and thus to passenger comfort. A measure of this

uniformity is the so-called uniformity index $\gamma$, which is defined as

$$\gamma = 1 - \frac{1}{2A\bar{v}_n} \cdot \int_{outlet} |v_n - \bar{v}_n| \, dA \,, \tag{4}$$

with $\bar{v}_n$ and $A$ being the average normal velocity in the outlet plane and the outlet cross sectional area, respectively. A value of $\gamma = 1$ corresponds to a fully uniform outflow.

After implementing the uniformity index as the second cost function, the resulting adjoint code was applied to the 3D air duct segment of Fig. 4. As can be seen from a comparison of Figs. 4 and 5a, the sensitivities wrt. dissipated power and uniformity index are quite contradictory. This does not come as a surprise: The cells along streamlines of high velocity are essential for the throughput of the channel. Its energetic efficiency would therefore strongly deteriorate if some finite porosity was added to these cells. On the other hand, in order to improve the flow *uniformity*, it is exactly these high-velocity cells that have to be slowed down by increasing their porosity.

As in the actual design process, a sensible trade-off between these two competing objectives can be obtained by a weighted sum of both objective functions. Fig. 5 therefore shows the combined sensitivity corresponding to

$$E/E_0 - \gamma \,, \tag{5}$$

where $E$ is normalized to its value for the zero porosity case $E_0$. Still for this combined sensitivity, the backflow areas are identified as counterproductive. The contribution of $\gamma$ to the combined cost function, however, makes a remarkable difference as compared to the pure $E$-sensitivities of Fig. 4: An guide plate appears close to the outlet plane, which aids in distributing the flow more equally across the outlet cross section.

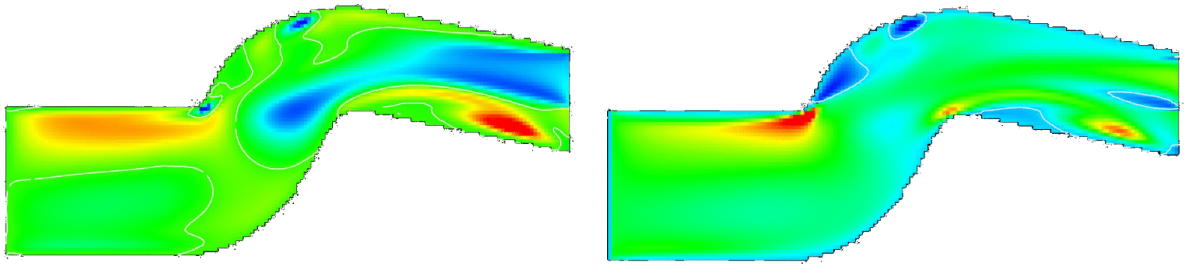

(a) (b)

Figure 5: Uniformity index test case: (a) Sensitivities of the air duct segment wrt. flow uniformity in the outlet plane. (b) Combined sensitivity of uniformity index and dissipated power. Note the appearance of the guide plate in front of the outlet.

Such an information is of enormous help for the engineer, who otherwise would have no idea of where to put such a baffle and how it should look like. Moreover, the appearance of the baffle constitutes a change in the *topology*, whereas apparently good-natured objective functions like dissipated power did – strictly speaking – not give rise to topology changes but only to shape modifications. This underlines the demand for a *topology* optimization methodology also in CFD.

### 3.3 Equal mass flow

Another commonly encountered problem in air duct design is to obtain a specific mass flow ratio between different outlets. Without appropriate optimization techniques, the engineering solution is to reduce in a trial-and-error fashion the cross section of those outlets that carry too much mass flow. This is neither an efficient procedure nor the best solution in terms of the incurred energetic dissipation.

In order to verify if our topology optimization method also serves for this kind of problems, we implemented the cost function "equal mass flow through both outlets", i. e. $|\dot{m}_1 - \dot{m}_2|$ into the code and applied it to the 2D test geometry of Fig. 6. At a Reynolds number of 1000, the fluid enters on the top left and leaves the domain through two different outlets on the right hand side: one exactly opposite to the inlet, and the other one shifted further down. At the inlet, the velocity was prescribed, whereas at the outlets, the static pressure was set to zero.

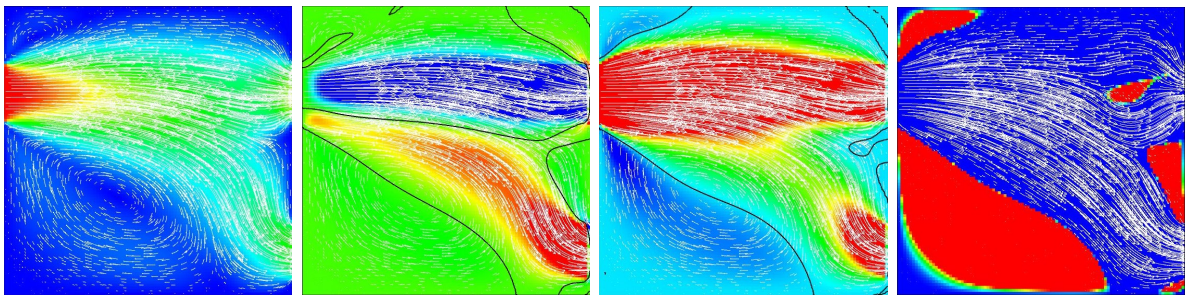

(a) (b) (c) (d)

Figure 6: Equal mass flow test case: (a) Initial velocity field (colours indicate the velocity magnitude), (b) sensitivities wrt. mass flow equality, (c) sensitivities wrt. dissipated power, (d) porosity distribution and velocity field after one iteration. Isolines of zero sensitivity are shown as black contours.

Obviously, the top outlet has the edge on the bottom one in terms of outgoing mass flow, the actual mass flow ratio being $\dot{m}_{top} : \dot{m}_{bottom} = 1.8 : 1$ for the original configuration. If we now compute the sensitivities wrt. to equal mass flow, the resulting distribution has a very straightforward interpretation (Fig. 6b): All the cells along the flow path towards the top outlet are "bad", because they contribute to the mass flow inequality, whereas all the cells on the way to the bottom outlet are "good".

Punishing the flow towards the top outlet according to this sensitivity field would correspond to the engineering solution described above, but, as also stated above, from an energetic viewpoint, this would certainly not generate the best solution. Our methodology, however, allows to take into account also the sensitivities of this configuration wrt. dissipated power (Fig. 6c) and to base an improved geometry on an appropriate combination of both objectives: equal mass flow *and* low dissipated power, in this case in equal terms according to $|\dot{m}_1 - \dot{m}_2|/|\dot{m}_1 + \dot{m}_2| + E/E_0$. The result of the first iteration of this procedure is shown in Fig. 6d, where the new geometry was obtained by setting the porosity in all cells of positive sensitivities to a high, practically blocking value. Instead of simply obstructing the way to the top outlet, aerodynamically formed guide plates appear, similar to the test case of the last subsection. They direct the fluid in favour of equalizing the outlet mass flows and, after this first iteration, generate a mass flow ratio of 1:0.9 and also reduce the dissipated power by roughly 15%.

### 3.4 Angular momentum

If appropriate objective functions are at hand, the proposed topology optimization methodology is, of course, not restricted to the design of air channels for cabin ventilation. Another field of application is the drafting of intake port geometries, with the most relevant cost function being the angular momentum of the flow in the outlet plane. A high angular momentum, or swirl motion, is desirable in view of the mixing of of air and fuel inside the combustion chamber. As the final application of this paper, we therefore tackle the problem of increasing the angular momentum of the flow in the outlet plane.

Fig. 7a illustrates the test geometry: The fluid enters a 3D box through the greenish rectangle, takes up some anglar momentum by flowing around a corner and then streams downwards into a quadratic channel. The left figure pair of Fig. 7b shows the streamlines of the original configuration (top) and the tangential velocity field in the outlet plane, which determines the swirl value. Two competing vortices are visible: a stronger with a clockwise rotation and a slightly weaker that rotates anti-clockwise.

How the flow looks like after one iteration is displayed by the right pair of Fig. 7b: At the cost of the anti-clockwise vortex, the area covered by the clockwise vortex has grown significantly, and the velocities associated with it have increased, thus giving rise to a swirl increase of roughly 100%.

Fig. 8 finally shows which geometric modification has generated the massive cost function improvement: The most prominent sensitivities were located within a curved baffle in the top half of the 3D box. The shape and position of the baffle enhances the effect of the corner of the original geometry, i. e. the picking up of angular momentum by the fluid.

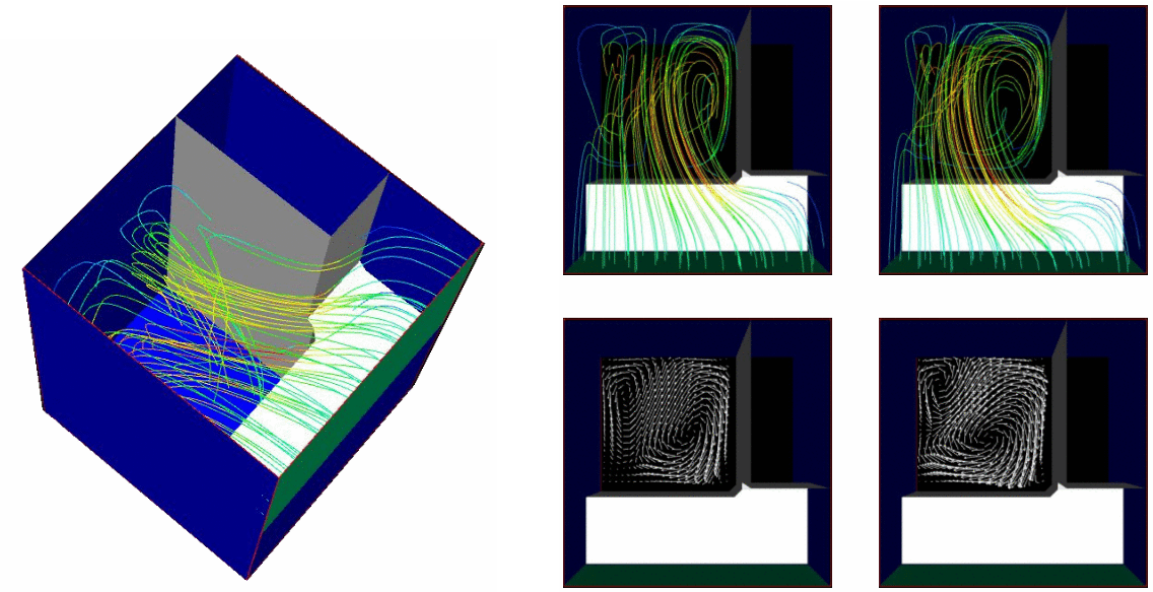

(a) (b)

Figure 7: Angular momentum test case: (a) Geometry: The fluid enters the box through the greenish plane. (b) Top view onto the geometry: Streamlines (top) and footprint (bottom) for the original geometry (left pair) and after one iteration (right pair). Note the growth of the clockwise vortex.

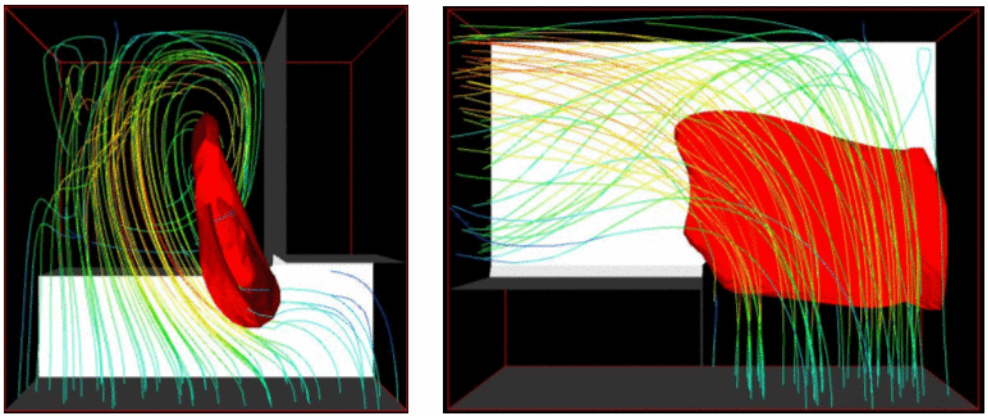

Figure 8: Angular momentum test case: Streamlines after one iteration as a result of the appearance of a curved baffle (left: top view, right: side view).

## 4 CONCLUSIONS

Two approaches to fluid dynamic topology optimization were presented: a pragmatic one and a second one based on adjoints. In both approaches, the geometry is controlled via continuous individual cell porosities. The pragmatic approach identifies counterproductive cells via a comparison of the actual flow field with the corresponding potential flow. It produces good results for 2D and 3D geometries and is very quick. However, as its net effect is the removal of backflow regions, it is limited to cost functions like dissipated power or pressure drop.

Our adjoint-based approach, which relies on sensitivities computed via adjoint states, overcomes this limitation: It can be trimmed to any thinkable cost function. With the help of automatic differentiation, we obtained a proof of concept of discrete adjoint-based topology optimzation. We focussed on the computation of sensitivities itself and were able to verify the applicability of the proposed methodology to diverse objective functions, which are relevant for the design of air ducts and intake ports.

The results look very promising, and part of our current work is actually dedicated to the implementation of this method into a professional CFD environment [9].

## REFERENCES

[1] M.P. Bendsøe and O. Sigmund, Topology optimization: theory, methods, and applications, Springer, Berlin, 2004.

[2] T. Borrvall and J. Petersson, Topology optimization of fluids in Stokes flow, *Int. J. Num. Meth. Fluids*, **41**, p. 77, 2003.

[3] O. Sigmund, A. Gersborg-Hansen, and R.B. Haber, Topology optimization for multiphysics problems: A future FEMLAB application?, *Proc. Nordic MATLAB Conf. 2003*, L. Gregersen (Ed.), Comsol A/S, Sborg, Denmark, p. 237, 2003.

[4] L.H. Olesen, F. Okkels, and H. Bruus, Topology optimization of Navier-Stokes flow in microfluidics, *ECCOMAS 2004*, Jyväskylä, 2004.

[5] O. Moos, F.R. Klimetzek, and R. Rossmann, Bionic optimization of air-guiding systems, *SAE 2004-01-1377*, 2004.

[6] J.K. Guest and J.H. Prévost, Topology optimization of creeping flows using a Darcy-Stokes finite element, *Int. J. Num. Meth. Engng.*, **66** (3), p. 461, 2006.

[7] M. Hassine, S. Jan, and M. Masmoudi, From differential calculus to 0-1 optimization, *ECCOMAS 2004*, Jyväskylä, 2004.

[8] S. Amstutz, Topological sensitivity in fluid dynamics, *ECCOMAS 2004*, Jyväskylä, 2004.

[9] C. Othmer, Towards an adjoint-based design process chain comprising topology and shape optimization, *ECCOMAS CFD 2006*, Delft, 2006.

[10] C. Othmer and Th. Grahs, Approaches to fluid dynamic optimization in the car development process, *EUROGEN 2005*, Munich, 2005.

[11] nav2df90, http://www.math.jmu.edu/∼dpruett/software/

[12] M. Griebel, T. Dornseifer, and T. Neunhoeffer, *Numerical Simulation in Fluid Dynamics, A Practical Introduction*, SIAM, Philadelphia, 1998.

[13] R. Giering and Th. Kaminski, Recipes for Adjoint Code Construction, ACM Trans. Math. Software **24**, p. 437, 1998.

[14] Th. Kaminski, R. Giering, and C. Othmer, Topological design based on highly efficient adjoints generated by automatic differentiation, *ERCOFTAC Design Optimization Conf.*, Las Palmas, 2006.